



Published in final edited form as:

Nat Biotechnol. ; 29(6): 505–511. doi:10.1038/nbt.1855.

Dosage suppression genetic interaction networks enhance functional wiring diagrams of the cell

Leslie Magtanong^{1,2,5,6}, Cheuk Hei Ho^{1,2,6}, Sarah L Barker^{1,2,6}, Wei Jiao^{1,2}, Anastasia Baryshnikova^{1,2}, Sondra Bahr^{1,2}, Andrew M Smith^{1,2}, Lawrence E Heisler², John S Choy³, Elena Kuzmin^{1,2}, Kerry Andrusiak^{1,2}, Anna Kobylanski², Zhijian Li^{1,2}, Michael Costanzo^{1,2}, Munira A Basrai³, Guri Giaever^{1,2,4}, Corey Nislow^{1,2}, Brenda Andrewa^{1,2}, Charles Boone^{1,2}

¹Department of Molecular Genetics, University of Toronto, Toronto, Ontario, Canada

²Banting and Bast Department of Medical Genetics, Terrence Donnelly Center for Cellular and Biomolecular Research, University of Toronto, Toronto, Ontario, Canada

³Genetic Branch Center for Cancer Research, National Cancer Institute, National Institutes of Health, Bethesda, Maryland, USA

⁴Department of Pharmaceutical Sciences, University of Toronto, Toronto, Ontario, Canada

⁵Present address: Howard Hughes Medical Institute, Department of Microbiology and Immunology, Albert Einstein College of Medicine, Bronx, New York, USA

⁶These authors contributed equally to this work

Abstract

Dosage suppression is a genetic interaction in which overproduction of one gene rescues a mutant phenotype of another gene. Although dosage suppression is known to map functional connections among genes, the extent to which it might illuminate global cellular functions is unclear. Here we analyze a network of interactions linking dosage suppressors to 437 essential genes in yeast. For 424 genes, we curated interactions from the literature. Analyses revealed that many dosage suppression interactions occur between functionally related genes and that the majority do not overlap with other types of genetic or physical interactions. To confirm the generality of these network properties, we experimentally identified dosage suppressors for 29 genes from pooled populations of temperature-sensitive mutant cells transformed with a high-copy molecularly barcoded open reading frame library, MoBY-ORF 2.0. We classified 87% of the 1,640 total

Correspondence should be addressed to C.B. (Charlie.boone@utoronto.ca) or B.A. (brenda.andrews@utoronto.ca).

AUTHOR CONTRIBUTIONS

L.M. was involved in MoBY-ORF construction, carried out experimental analysis and wrote the manuscript; C.H.H. was involved in MoBY-ORF construction, carried out experimental analysis and wrote the manuscript; S.L.B. was involved in MoBY-ORF construction and wrote the manuscript; W.J. and A.B. carried out computational analysis and wrote the manuscript; S.B. was involved in temperature-sensitive strain generation and carried out experimental analysis; A.M.S. and L.E.H. were involved in microarray data analysis; J.S.C. carried out the chromosome loss assays; E.K. and K.A. carried out experimental analysis and edited the manuscript; A.K. carried out experimental analysis; Z.L. was involved in temperature-sensitive strain generation; M.C. wrote the manuscript; M.A.B. edited the manuscript; G.G. and C.N. provided microarray data analysis and edited the manuscript; B.A. wrote the manuscript; C.B. conceived and planned the construction of the MoBY-ORF 2.0 library and wrote the manuscript.

COMPETING FINANCIAL INTERESTS

The authors declare no competing financial interests.

Accession codes. Microarray data have been deposited in ArrayExpress under accession code E-TABM-1147.

Note: Supplementary information is available on the Nature Biotechnology website.

Interactions into four general types of suppression mechanisms, which provided Insight into their relative frequencies. This work suggests that Integrating the results of dosage suppression studies with other Interaction networks could generate insights into the functional wiring diagram of a cell.

Increasing gene dosage provides a means of probing gene function as it tends to cause an increase in gene activity called a gain-of-function effect^{1,2}. Gene overexpression is relevant to the molecular mechanisms of diseases such as cancer, in which gene amplification and gain-of-function mutations are implicated in disease initiation and progression³. In wild-type yeast cells, systematic analysis of gene overexpression has revealed that only a subset of genes cause an overt phenotype when overexpressed ectopically^{1,2,4-6}. However, examining gene overexpression in sensitized cells containing mutations in genes of known function is an effective way to probe gene activity^{2,7-10}, demonstrating that gene dosage studies identify functionally relevant genetic interactions. Despite their functional utility, systematic dosage suppression and the relationships between it and other types of interactions have been largely unexplored.

Genetic interaction networks map functional connections occurring both within and between cellular pathways. An extensive genetic interaction network based on loss-of-function double mutant analysis has been described for budding yeast¹¹. This quantitative genetic network maps both negative and positive genetic interactions, scoring an interaction when the double mutant is either less or more fit than expected on the basis of the combined effect of the single mutations¹², in addition to the genetic network, a large-scale physical interaction network for yeast has been assembled from multiple data sources¹³⁻¹⁶. Direct interactions between genes or gene products are called 'edges' in biological network graphs. The edges in the genetic interaction network largely complement those found in the protein-protein interaction network, as only a small fraction of gene pairs that show a genetic interaction also physically interact¹¹. Thus, an integrated network is more informative than either individual network¹⁷. Despite the mapping of these genome-scale networks, our knowledge of the cell remains incomplete, and thus systematic identification and subsequent integration of new types of genetic interactions should provide further insight into the roles of specific genes and improve our global understanding of the functional wiring diagram of the cell.

Rescue of a mutant phenotype through overexpression of a gene is called dosage suppression. This type of genetic interaction has been examined in many diverse studies, often using an allele of an essential gene that has a temperature-sensitive growth defect⁸—that is, an exaggerated mutant phenotype is observed at a higher, restrictive temperature. In many cases, overexpression of the dosage suppressor allows the mutant cells to grow normally at a semipermissive temperature. For example, overexpression of the genes encoding either Cdc42p or Rsr1p, the Rho-related or Ras-related GTPases, respectively, suppresses a temperature-sensitive allele of *CDC24* (ref. 18), which encodes the guanine nucleotide exchange factor for Cdc42p that seems to be activated by Rsr1p signaling¹⁹. Studies such as these have shown that dosage suppression analysis can delineate the architecture of signaling pathways and identify novel pathway components, but the potential

value of systematically mapping these interactions has not been examined. To address this issue, here we analyze properties of dosage suppression interaction networks and develop reagents that facilitate high-throughput mapping of dosage suppression interactions in the yeast *Saccharomyces cerevisiae*.

RESULTS

A global dosage suppression genetic interaction network

We collected a set of dosage suppression genetic interactions for 424 essential genes, which we call ‘query’ genes, that were annotated in the *Saccharomyces* Genome Database (SGD, <http://www.yeastgenome.org/>; Supplementary Table 1). These interactions form a network containing 768 genes and 1,293 interactions (Fig. 1 and **Supplementary Data**). Most query genes have only a few dosage suppressors, although a small set of genes has a large number of interactions (Supplementary Fig. 1 and Supplementary Table 1).

The network was visualized in Cytoscape using a force-directed layout²⁰, such that genes sharing common dosage suppression interactions formed distinct clusters. Markov clustering analysis²¹ identified nine clusters, each containing ~30 genes that correspond to specific biological processes. Similar to the synthetic genetic network¹¹, the relative distance between these clusters seems to reflect shared functionality (Fig. 1). For example, the functional relationships among vesicle-mediated transport, exocytosis and cell growth and morphogenesis are indicated by the relatively close proximity of their corresponding gene clusters in the network, along with a substantial number of dosage suppression interactions that occur between genes functioning in these different processes. This suggests that dosage suppression interactions, like other forms of genetic interactions^{10,11}, can be used to independently cluster genes on the basis of functional interrelatedness.

Dosage suppressor distribution across cellular processes

We examined the occurrence of dosage suppression genetic interactions within and across different cellular processes. Consistent with the connectivity of other biological networks^{11,13–16}, we found that genes involved in the same biological process were highly enriched for dosage suppression interactions. Notably, we also observed a substantial number of dosage suppression interactions between distinct yet related processes (Fig. 2a). For example, the growth defects of strains containing mutations in cell polarity and morphogenesis pathways are suppressed by overexpression of genes involved in several different functional categories, including those that act at various steps in intracellular vesicle-mediated transport. Thus, dosage suppression interactions can map phenotypic connections between functionally diverse genes.

Dosage suppression overlaps with other network edges

We explored the overlap of dosage suppression genetic interactions with three other interaction networks: the physical (protein-protein)^{13–16}, negative genetic and positive genetic networks¹¹. We found that the dosage suppression network was enriched significantly ($P \ll 10^{-16}$) for both physical and negative genetic interactions but not for positive genetic interactions ($P = 0.52$) (Table 1). Despite this overlap with physical and

negative genetic interactions, most dosage suppression interactions (68%) did not overlap with any previously mapped network edge (Fig. 2b and Supplementary Table 1). Notably, these unique dosage suppression interactions were enriched for gene pairs that shared gold-standard Gene Ontology terms²² (55%; $P \ll 10^{-16}$). Thus, dosage suppression seems to often identify a type of interaction capable of covering novel network space.

Systematic dosage suppression analysis with MoBY-ORF 2.0

Because the literature-curated network could be based on selected results and therefore biased, we carried out a systematic dosage suppression analysis on a subset of functionally diverse genes. Classic gene dosage suppression studies in yeast have been carried out productively using high-copy libraries of plasmids carrying random genomic fragments^{4,23}; however, the fragments in these libraries are often large, meaning that the suppressing gene must be identified through an additional round of experiments. For more efficient analysis, we developed a high-copy plasmid library (based on the yeast 2 μ plasmid) in which each plasmid contains a DNA insert composed of a single yeast open reading frame (ORF) with its native upstream and downstream genomic sequences, along with two unique 20-nucleotide molecular barcode tags (Supplementary Fig. 2). The 2 μ -based molecular ular barcoded yeast ORF (MoBY-ORF 2.0) plasmid library provides a reagent set tailored for gene dosage analysis because the abundance of a dosage suppressor gene can be monitored in a pool of transformants using a barcode-microarray readout.

We also developed a protocol for identifying dosage suppressors of conditional temperature-sensitive alleles of essential genes (Supplementary Fig. 3). Briefly, mutants are transformed with the MoBY-ORF 2.0 library, and transformants carrying either dosage suppressors or a wild-type copy of the essential gene (which complements the temperature-sensitive mutation, *ts*) are selected on solid medium at a semipermissive temperature. Then, barcodes derived from the pool of selected cells are amplified by PCR and competitively hybridized with those of a control preselection pool to a barcode microarray. Candidate dosage suppressors are identified by the fact that their barcodes have raw hybridization intensity significantly above background (Supplementary Fig. 4). To confirm dosage suppression interactions, candidate dosage suppressor plasmids are individually transformed into the cognate temperature-sensitive strain, and spot dilutions are carried out at the semipermissive temperature.

We used this protocol to screen for suppressors of 41 query genes that participate in a variety of cellular processes including, but not limited to, protein degradation (*RPN11*), secretion (*SEC17*, *SEC18* and *SEC26*), transcription (*CCL1* and *MED4*) and chromosome segregation (*SCC4*, *NSL1* and *DSN1*) (Supplementary Table 2). The majority of the query genes had relatively few or no previously published dosage suppression interactions (Supplementary Table 1).

We carried out confirmation transformations and spot dilution assays to validate 214 different suppressing plasmids (Supplementary Table 2), which represent 23% of the dosage suppressors identified in the initial screens. The relatively low confirmation rate may be attributed, in part, to how we harvested the candidate suppressor colonies. This procedure involved washing the plates completely, and therefore may include some general background

colonies. However, despite differences in screening conditions and genetic backgrounds, we identified 6/10 (60%) of previously reported literature-curated interactions for the 41 query genes (Supplementary Table 2). Notably, the wild-type complementing ORF was recovered for all but three query strains. We expected a few cases in which we would not observe complementation because the 2 μ MoBY-ORF library does not contain wild-type plasmids for ~20% of yeast ORFs, including those of these three strains, and most (~93%) but not all of the PCR-amplified genes are functional²⁴. Of the 168 extragenic dosage suppressors, three plasmid clones carried the wild-type complementing ORF in addition to genes immediately next to it (Supplementary Table 2). As each MoBY-ORF 2.0 plasmid carries native upstream and downstream ORF sequence, two ORFs can occur on a single plasmid if the intergenic region is relatively small. For several query genes, we screened multiple alleles and recovered the same suppressor gene.

The number of dosage suppressors varied widely from 0—that is, recovery of only the wild-type gene—to 24 (Supplementary Fig. 1 and Supplementary Table 2), but on average, we recovered ~5 dosage suppressors per query gene. In total, we found 137 previously unreported dosage suppression interactions for 29 query genes, including 13 query genes that had no previously known dosage suppressors (Supplementary Tables 1 and 2).

Similar to what we observed for the literature-curated dosage suppression network, a significant portion (~40%, $P < 2.6 \times 10^{-10}$) of these 137 dosage suppression interactions linked pairs of genes annotated with the same Gene Ontology term²² (Supplementary Tables 1 and 2), suggesting that the dosage suppressors are functionally related to their respective query genes. Moreover, our dosage suppression interactions overlapped significantly with protein-protein interactions and negative genetic interactions but not with positive genetic interactions; however, most edges were unique (Table 1). On the basis of these observations, we conclude that the literature-curated network represents the general properties of the global suppression network and, notably, our systematic analysis confirms that the majority of dosage suppression interactions cover relatively unexplored and functionally relevant network space.

Dosage suppression links PKA signaling and Kinetochores function

A detailed examination of specific dosage suppression interactions can provide new mechanistic insight into particular pathways and complexes¹⁸. In particular, the regulatory targets of signaling pathways can be revealed by dosage suppression interactions. For example, in our systematic analysis, we screened two components of the essential Mtw1p including the Nnf1p-Nsl1p-Dsn1p (MIND) kinetochores complex (Fig. 3a), which participates in bridging centromeric heterochromatin and kinetochores microtubule-associated proteins (MAPs) and motors^{25,26}. Although dosage suppressors have not been mapped previously for *NSL1* or *DSN1*, we identified a subnetwork of 31 interactions and 28 genes impinging on these two query genes (Supplementary Table 2). Among the dosage suppressors we identified for both *NSL1* and *DSN1* were the S-phase transcription factor HCM1 and a ribosomal biogenesis gene, *FCF1*. *HCM1* has been predicted to directly upregulate transcription of both *NSL1* and *DSN1* (ref. 27), and *ns11(ts) hcm1* and *dsn1(ts) hcm1* double mutants each show a negative genetic interaction¹¹; therefore, our results are

consistent with both the *in silico* predictions and the double mutant phenotypes. We also identified *SPC105* as a *DSNI* dosage suppressor. Spc105p forms a complex with Kre28p, and this complex also acts as an essential kinetochore linker complex²⁶.

Two redundant genes that downregulate protein kinase A (PKA) signaling at various steps in the pathway, *GPB1* and *GPB2*, were also identified as dosage suppressors of *DSNI* (Fig. 3a). A third gene, *GIS2*, is not well characterized but is thought to act as a negative regulator, similar to *PDE2*, in PKA signaling²⁸. Although a genetic link between the PKA pathway and the Dam1p-Duo1p (or DASH) kinetochore and microtubule-associated complex has been observed²⁹, our results identify a functional relationship between downregulation of PKA signaling and the MIND complex. Thus, our results support a model in which attenuation of PKA signaling contributes to proper kinetochore function.

Because overexpression of negative regulators of the PKA pathway suppresses the temperature-sensitive mutant phenotypes of *DSNI* and DASH complex–encoding genes²⁹ and because temperature-sensitive alleles of kinetochore genes are often associated with a chromosome loss phenotype³⁰, we hypothesized that hyperactive PKA signaling may also lead to a chromosome loss phenotype. To test this possibility, we deleted *BCY1*, a negative regulator of cAMP-protein kinase³¹, in a diploid query strain that enables a quantitative analysis of chromosome loss frequencies³². Indeed, we found that heterozygous *bcy1* / *BCY1* diploids showed a pronounced chromosome loss phenotype compared with the wild-type diploid control (Fig. 3b). Thus, we suspect that PKA signaling may act to provide rheostat-like control over MIND and DASH kinetochore functions, in which increased signaling antagonizes kinetochore activity and decreased signaling potentiates it.

Mechanistic categories of dosage suppression interactions

A general mechanistic categorization of second-site genetic suppression has been described^{9,33}. To extend this analysis to dosage suppression genetic interactions and to explore the frequency with which each of the mechanisms is observed genome-wide, we developed a decision tree for classifying dosage suppression genetic interactions in yeast into four general mechanistic categories (Fig. 4). We used the tree to analyze the integrated network of interactions curated from the literature and observed experimentally in this work, classifying 1,422 of 1,640 (87%) of the dosage suppression interactions into one of the four categories, with the mechanism underlying the remaining interactions (13%) classified as unknown (Fig. 4; Supplementary Tables 1 and 2).

The decision tree first classified 1,285/1,640 (~80%) of all pairs of genes linked by dosage suppression interactions as being functionally related because they were annotated with the same Gene Ontology term within a gold-standard set of terms²² (Supplementary Tables 1 and 2). We considered two mechanisms that may explain dosage suppression interactions between genes in the same general biological pathway or process (Fig. 5a,b).

The first mechanistic category of dosage suppression is ‘complex component,’ defined as dosage suppression interactions between genes annotated with the same Gene Ontology term whose gene products are also linked by a physical protein-protein interaction (Fig. 5a). This category contained 525 interactions. Classical examples of genes in this category include the

G1 cyclins *CLN1* and *CLN2*, which were initially discovered as dosage suppressors of *cdc28-1*, a temperature-sensitive allele of the essential gene encoding the cyclin-dependent kinase Cdc28p³⁴. Subsequent studies have shown that the cyclins bind to and activate Cdc28p³⁵. A direct physical interaction between a mutant query gene product and its dosage suppressor may also indicate that the dosage suppressor can stabilize a protein complex containing the query mutant protein. On the basis of this hypothesis and because essential genes tend to form complexes containing other essential genes, reciprocal dosage suppression (in which gene *A* suppresses query mutant *b* and gene *B* suppresses query mutant *a*) may be expected between two essential gene products belonging to the same protein complex. We identified 28 dosage suppression interactions in our screens in which both the query mutant and the dosage suppressor were essential (Supplementary Table 2). Of the 28 gene pairs, 9 showed reciprocal dosage suppression (Supplementary Table 3), such that growth defects associated with mutations in either gene could be suppressed by overexpressing its partner. Notably, all nine gene pairs also shared a physical interaction among their gene products; it is highly improbable that this occurred by chance (Supplementary Table 3; $P \ll 10^{-16}$). Similarly, 75% of reciprocal dosage suppression interactions reported in the literature also share a physical interaction (Supplementary Table 4). Thus, the strong overlap between reciprocal dosage suppression and physical interactions provides evidence supporting a mechanism in which phenotypic suppression is mediated by increased stability of the protein complex.

The second mechanistic category included the remaining 760 ‘functionally related’ genes that show dosage suppression interactions without physical interactions (Fig. 5b). For example, mutations in *SEC3*, which encodes an essential member of the exocyst complex that transports secretory vesicles from the trans-Golgi network to the plasma membrane, are suppressed by overexpression of either of two functionally redundant plasma membrane t-SNAREs, *SSO1* and *SSO2*, involved in the fusion of secretory vesicles to the plasma membrane³⁶. Dosage suppression interactions have also been identified among duplicated genes and gene pairs that share the same molecular function (Supplementary Table 1); in both cases, the biochemical activity of the dosage suppressor can functionally substitute for the mutant gene product⁸.

The third mechanistic category is ‘chaperone suppressor,’ which applied to a subset of 15 dosage suppression interactions between genes annotated as participating in different biological processes. Chaperones, such as heat-shock proteins (HSPs) or RNA stability factors, can act as dosage suppressors by stabilizing the levels of a query gene product (Fig. 5c). Indeed, increased dosage of HSPs suppressed diverse sets of genes that do not share any obvious functional relationship (Supplementary Tables 1 and 2).

The fourth mechanistic category applied to 104 interactions involving genes encoding ribosomal subunits and RNA processing factors, which were identified as dosage suppressors for a variety of query genes (Supplementary Tables 1 and 2). Although the molecular mechanisms of dosage suppression in these cases are not well understood, increased dosage of the suppressing genes may lead to increased transcription or translation of the product of the temperature-sensitive query gene (Fig. 5d), thereby compensating for a *ts* mutation that represses transcription of RNA processing and/or ribosomal subunit genes.

For example, transcriptional profiling of *myo1* cells, which lack the lone copy of the type II myosin heavy chain in the yeast genome³⁷, has shown downregulation of many genes, including several ribosomal subunit genes³⁸, and overexpression of some of these genes can rescue the associated mutant phenotypes (Supplementary Table 1). We found that a relatively small fraction (7%) of dosage suppression interactions belonged in the chaperone and RNA processing/ ribosome category.

We assigned the remaining 236 interactions to the ‘unknown’ category. Notably, within this category, we identified several (14) dosage suppression gene pairs whose protein products have a known physical interaction but whose genes do not share any gold-standard Gene Ontology terms in common (Supplementary Table 1). For every interaction initially placed in the unknown category, including gene pairs both with and without known physical interactions between their gene products, we revisited the primary literature in an effort to find other functional information that might support reclassification of a particular interaction into a mechanistic category. By doing so, we reclassified 10% of the unknown interactions into one of the other mechanisms of dosage suppression.

DISCUSSION

Global mapping of dosage suppression genetic interactions derived from literature-curated data generated a coherent network of functional relationships among genes (Fig. 1). Indeed, mechanistic classification of the dosage suppression interactions revealed that the vast majority of dosage suppression interactions (~80%) occur between functionally related genes (Fig. 5). Most dosage suppression interactions capture relationships that are not observed by other methods, as only 32% overlap with protein-protein and negative genetic interactions. Thus, dosage suppression defines a distinct type of network edge, whose integration with other global data sets should enhance a functional wiring diagram of the cell.

The observation that some dosage suppression interactions overlap with protein-protein interactions (Table 1 and Supplementary Tables 1, 2 and 5) supports the hypothesis that a direct interaction between a mutant query gene product and its dosage suppressor may stabilize a complex containing the query mutant protein³⁴. We also found that a significant fraction of dosage suppression genetic interactions overlap with negative genetic interactions. A negative genetic interaction is defined as a double-mutant fitness defect that is statistically significantly stronger than expected, given the two single mutant fitness defects^{10,12,39}. This observation is consistent with the overlap with protein-protein interactions because genes whose products interact within an essential complex often show negative genetic interactions¹². In the context of dosage suppression, the fitness of the query mutant is improved by overexpressing the wild-type copy of an interacting gene, whereas in the context of a negative genetic interaction, the fitness defect of the mutant is enhanced by a loss-of-function allele of the interacting gene.

In contrast, we did not observe a statistically significant overlap between positive genetic interactions and dosage suppression network edges (Table 1). Positive genetic interactions occur when a double mutant shows a fitness defect that is less severe than expected on the

basis of the fitness of the corresponding single mutants^{10,12,39}. A subset of positive genetic interactions occurs between genes whose products form a nonessential physical complex. We would not expect these positive interactions to overlap with our dosage suppression interactions because all of the query genes on the dosage suppression network are essential genes. Another subset of positive interactions are those in which the loss of function of one gene suppresses the fitness defect associated with loss of function of another gene^{12,40}. Gene overexpression typically leads to gain-of-function phenotypes, although in rare instances increased gene dosage can lead to dominant-negative (loss-of-function) phenotypes², and thus we do not expect a strong overlap with positive genetic interactions.

The results of our systematic dosage suppression screens suggested that the network properties associated with the literature-curated dosage suppression network are not biased and, in fact, represent general features of dosage suppression networks. However, the mechanistic classification of dosage suppressors revealed that RNA processing and protein synthesis genes represented a larger fraction of dosage suppressors in our systematic analysis than in the literature (25% versus 5%; Supplementary Tables 1 and 2). We expected to identify RNA processing and protein synthesis suppressors because the heat stress associated with exposure of temperature-sensitive mutants to a restrictive temperature induces a general and transient decrease in expression of genes involved in RNA processing and protein synthesis⁴¹. Moreover, some ts mutations may lead specifically to defects in different steps of protein synthesis, protein folding or, in the case of protein complexes, the protein assembly process⁴². In some cases, however, the suppression may be pathway-specific because some ribosomal paralogs have specialized roles, and extraribosomal functions for ribosomal genes have been reported^{43–45}. Furthermore, we suspect that our unbiased screen may identify more RNA processing and protein synthesis genes as suppressors simply because these genes may be omitted from focused studies that only include what the authors consider functionally relevant results.

Conditional alleles are being developed for the majority of essential genes in yeast^{46,47}, and thus a dosage suppression genetic interaction network could be mapped for the entire spectrum of essential genes. This mapping effort could extend to the majority of nonessential genes on the dosage suppression network through the creation of temperature-sensitive alleles of each gene within the context of a synthetic lethal background¹¹. With about five dosage suppression interactions per query gene, the dosage suppression network offers the potential of new functional information and connections. Although we demonstrate the utility of this type of genetic interaction in yeast, an analogous mapping of genetic interactions should be possible in mammalian cells and metazoan model systems. We conclude that a global dosage suppression map adds a highly prevalent and distinct type of functional ‘edge’ that could be integrated into the construction of a complete cellular landscape comprising all types of genetic and physical interactions.

METHODS

Methods and any associated references are available in the online version of the paper at <http://www.nature.com/nbt/index.html>.

ONLINE METHODS

Identifying gene clusters in the dosage suppression genetic interaction network

The network was clustered using the Markov clustering algorithm²¹. Nine clusters containing >30 genes were tested for functional enrichment using the BiNGO plugin for Cytoscape⁴⁸. The Gene Ontology biological process term with the highest enrichment in a particular cluster was used to label the cluster on the network.

Overlap of dosage suppression genetic interactions with other types of interactions

The literature-curated dosage suppression data set and protein-protein interaction data set were downloaded from the SGD on 20 May 2010. Dosage suppression data were filtered to include only gene pairs containing an essential gene as the query ORE. The list of essential genes was downloaded from the *Saccharomyces* Genome Deletion Project database (http://www.sequence.stanford.edu/group/yeast_deletion_project/) on 20 March 2010.

Analysis of functional relatedness

Two genes sharing a dosage suppression interaction were considered to be functionally related if they were annotated to the same Gene Ontology term. Only Gene Ontology terms from a published gold standard were considered²². Gene Ontology annotations were downloaded from the SGD on 11 May 2010.

Growth media

Yeast strains were grown in SD —Leu (0.67% (wt/vol) yeast nitrogen base (Difco), 0.2% amino acid supplement minus Leu (Fisher), 2% (wt/vol) glucose) or SC (0.67% (wt/vol) yeast nitrogen base, 0.2% (wt/vol) amino acid supplement (Fisher), 2% (wt/vol) glucose) medium. Bacteria were grown in 2× YT medium (1% (wt/vol) yeast extract (Difco), 1.6% (wt/vol) tryptone (Difco), 0.5% (wt/vol) sodium chloride) or in YE medium (0.5% (wt/vol) yeast extract, 1% (wt/vol) NaCl).

MoBY-ORF 2.0 library clone construction using MAGIC

MoBY-ORF v1.0 bacterial strains²⁴ were inoculated from frozen stocks in 96-well plates into a shallow 96-well plate in which each well had 100 µl 2× YT medium containing 5 µg ml⁻¹ tetracycline, 50 µg ml⁻¹ kanamycin and 12.5 µg ml⁻¹ chloramphenicol. Cultures were grown for ~16 h at 37 °C. P5530 (genotype: *lacI^QrrnB3 lacZ4787 hsdR514 (araBAD)567 (rhaBAD)568 galU95 endA9:FRT recA635:FRT umuC:ParaBAD-I-SceI-FRT*), the MAGIC recipient strain carrying plasmid p5476 (Supplementary Fig. 5), was inoculated into 5 ml of YE +Gluc medium, containing 0.2% (wt/vol) glucose, 10 µg ml⁻¹ spectinomycin and 200 µg ml⁻¹ carbenicillin. Cultures were grown for ~22 h at 30 °C. The next day, we measured the A₆₀₀ values of the recipient strain and of three bacterial (donor) strains from the MoBY-ORF 96-well plate; the average of the three wells was used as the average A₆₀₀ for the entire plate. Cultures were diluted to A₆₀₀ ≈ 0.10 and mixed together forming in a 1:1 ratio in a total volume of 100 µl in a fresh 96-well plate. Cells were shaken at 30 °C for 2 h, at which time L-arabinose was added to a final concentration of 0.2% (wt/vol) to each well. Cells were incubated without shaking at 37 °C for 2 h and then transferred to a shaking

incubator at 37 °C for 2 h. Of the 100 µl mating reaction, 2 µl was plated onto YE +Glyc medium containing 0.2% glycerol (wt/vol), 0.2% (wt/vol) dL-chlorophenylalanine, 200 µg ml⁻¹ carbenicillin, 50 µg ml⁻¹ kanamycin and incubated at 41 °C overnight.

Mating products were streaked out for individual colonies onto 2× YT medium containing 0.2% (wt/vol) glucose, 200 µg ml⁻¹ carbenicillin and 50 µg ml⁻¹ kanamycin and incubated at 37 °C overnight. Miniprep DNA was prepared from a single bacterial colony, doubly digested using XhoI and EcoRI (Fermentas) and resolved on a 0.8% agarose gel to confirm vector and insert fragment sizes (Supplementary Table 6). Two individuals carried out gel analysis independently, and the results were compared to determine clone validity. If the primary XhoI-EcoRI digest was ambiguous, a secondary digest using BamHI and HindIII was carried out. ORF fragment sizes for both double digests, along with complete ORF sequence and barcodes, can be obtained from the MoBY-ORF database (<http://moby.ccb.utoronto.ca/>). The final MoBY-ORF 2.0 plasmid library contains 4,547 clones (representing 4,499 ORFs; Supplementary Table 7), of which 91% have two usable barcodes, 5% have a unique uptag only and 4% have a unique downtag only. The library will be available from Open Biosystems.

Plasmid pool preparation

Individual *Escherichia coli* transformants containing a barcoded high-copy plasmid were grown in 100 µl of 2× YT medium containing 0.2% (wt/vol) glucose, 200 µg ml⁻¹ carbenicillin and 50 µg ml⁻¹ kanamycin at 37 °C for 15 h in a shallow 96-well plate. A total of 55 µl of each culture was mixed to form the *E. coli* MoBY-ORF version 2.0 pool. Plasmid DNA was prepared from the *E. coli* pool.

Cloning of dosage suppressors with the MoBY-ORF 2.0 library

Each temperature-sensitive query strain (Supplementary Table 8) was transformed with MoBY-ORF v2.0; 50,000 transformants were pooled and frozen in 15% (wt/vol) glycerol. For identification of suppressors, a sample of the transformant pool was thawed, and 50,000 cells were plated onto SD -Leu. The incubation temperatures for each strain depended on the observed restrictive temperature for the untransformed temperature-sensitive mutant⁴⁷. For a given strain at a particular temperature, colonies that appeared after 3 d were pooled (to form the dosage suppressor pool) and stored at -80 °C in 15% (wt/vol) glycerol. To isolate suppressing plasmids, a sample of the dosage suppressor pool was thawed, and plasmids were isolated using a modified miniprep protocol of the Qiagen miniprep kit as described⁴⁹.

Yeast barcode microarray hybridization and data analysis

PCR amplification of the barcodes and TAG4 microarray hybridization were carried out as described⁵⁰. For each array, a competitive hybridization was carried out. Biotinylated universal TAG4 primers were used to PCR-amplify the barcodes from the dosage suppressor pool, whereas nonbiotinylated universal TAG4 primers were used to PCR-amplify the barcodes from the original transformant pool. Each hybridization mix contained 9:1 (vol/vol) nonbiotinylated/biotinylated PCR product. A raw microarray signal of 1,000 average fluorescence units (a.f.u.), determined empirically (Supplementary Fig. 4), was used as the cutoff for identifying candidate dosage suppressors.

Empirical determination of raw barcode microarray intensity cutoff for identification of candidate dosage suppressors

Cells (50,000) representing a pooled sample of the transformants of each strain were plated on selected medium and incubated at the semipermissive temperature. Colonies appearing after 3 d at the semipermissive temperature were individually picked and pooled. We anticipated that the plasmid pool contained in this mixture would identify a distinct set of barcodes with raw intensity signals greater than the observed microarray background cutoff (~30 a.f.u.) and thereby identify an empirical cutoff for candidate dosage suppressors. Barcoded plasmids were extracted from the pooled colonies, the barcodes were PCR amplified, and a competitive microarray hybridization was carried out as described.

For *cdc48-9*, 24 barcode signals were greater than the standard background. Using cutoffs of 2,000, 1,000 and 500, 14/24 (58%), 19/24 (80%) and 21/24 (88%) of the barcodes in the sample were retrieved, respectively.

For *nse3-ts5*, 6 barcode signals were greater than the standard background. Using cutoffs of 2,000, 1,000 and 500, 3/6 (50%), 4/6 (66%) and 4/6 (66%) of the barcodes in the sample were retrieved, respectively.

For *stu2-11*, 10 barcode signals were greater than the standard background. Using cutoffs of 2,000, 1,000 and 500, 4/10 (40%) 5/10 (50%) and 5/10 (50%) of the barcodes in the sample were retrieved, respectively.

Because for two of the three strains, there was no difference in the number of barcodes retrieved between the 500 and 1,000 raw intensity cutoffs, and for one strain, there was a marginal (<10%) difference, we decided to use the more stringent cutoff of 1,000 raw a.f.u. for identification of candidate dosage suppressors.

Confirmation of candidate dosage suppressors and test for reciprocal suppression

Individual 2 μ MoBY-ORF plasmids were transformed into the corresponding temperature-sensitive strain (Supplementary Table 8) using standard methods. Spot dilutions were carried out on SD -Leu medium using standard methods and incubated at the same temperature at which the dosage suppressor was initially identified (for candidate dosage suppressors) or the corresponding semipermissive temperature of the temperature-sensitive strain (for reciprocal suppression tests).

Chromosome loss rate measurements

Chromosome loss rate measurements were carried out as described^{32,51}, except that *HOM3* was replaced with *LEU2* on chromosome V. Measurements were carried out three independent times for wild type and *bcy1* /*BCY1*, and twice for *ctf19* /*ctf19* .

Supplementary Material

Refer to Web version on PubMed Central for supplementary material.

ACKNOWLEDGMENTS

We thank S. Dixon for critical comments on the manuscript, M. Gebbia for microarray technical support, and C. Myers and J. Bellay for advice and data analysis support. L.M. was supported by a Canadian Institutes of Health Research (CIHR) doctoral research award. A.M.S. was supported by a University of Toronto open fellowship. J.S.C. and M.A.B. were supported by the Intramural Research Program of the US National Cancer Institute, US National Institutes of Health. G.G. was supported by the Canadian Cancer Society and the CIHR (research agreements 020380 and MOP-81340, respectively). C.N. was supported by the CIHR (MOP-84305). C.B. and B.A. were supported by Genome Canada through the Ontario Genomics Institute (2004-OGI-3-01). C.B. was supported by the CIHR (MOP-57830) and the Natural Sciences and Engineering Research Council of Canada (RGPIN 204899-06).

References

1. Vavouri T, Semple JI, Garcia-Verdugo R & Lehner B Intrinsic protein disorder and interaction promiscuity are widely associated with dosage sensitivity. *Cell* 138, 198–208 (2009). [PubMed: 19596244]
2. Sopko R et al. Mapping pathways and phenotypes by systematic gene overexpression. *Mol. Cell* 21, 319–330 (2006). [PubMed: 16455487]
3. Santarius T, Shipley J, Brewer D, Stratton MR & Cooper CS A census of amplified and overexpressed human cancer genes. *Nat. Rev. Cancer* 10, 59–64 (2010). [PubMed: 20029424]
4. Jones GM et al. A systematic library for comprehensive overexpression screens in *Saccharomyces cerevisiae*. *Nat. Methods* 5, 239–241 (2008). [PubMed: 18246075]
5. Moriya H, Shimizu-Yoshida Y & Kitano H *In vivo* robustness analysis of cell division cycle genes in *Saccharomyces cerevisiae*. *PLoS Genet.* 2, e111 (2006). [PubMed: 16839182]
6. Kaizu K, Moriya H & Kitano H Fragilities caused by dosage imbalance in regulation of the budding yeast cell cycle. *PLoS Genet.* 6, e1000919 (2010). [PubMed: 20421994]
7. Boone C, Bussey H & Andrews BJ Exploring genetic interactions and networks with yeast. *Nat. Rev. Genet.* 8, 437–449 (2007). [PubMed: 17510664]
8. Rine J Gene overexpression in studies of *Saccharomyces cerevisiae*. *Methods Enzymol.* 194, 239–251 (1991). [PubMed: 2005790]
9. Prelich G Suppression mechanisms: themes from variations. *Trends Genet.* 15, 261–266 (1999). [PubMed: 10390624]
10. Dixon SJ, Costanzo M, Baryshnikova A, Andrews B & Boone C Systematic mapping of genetic interaction networks. *Annu. Rev. Genet.* 43, 601–625 (2009). [PubMed: 19712041]
11. Costanzo M et al. The genetic landscape of a cell. *Science* 327, 425–431 (2010). [PubMed: 20093466]
12. Baryshnikova A et al. Quantitative analysis of fitness and genetic interactions in yeast on a genome scale. *Nat. Methods* 7, 1017–1024 (2010). [PubMed: 21076421]
13. Gavin AC et al. Functional organization of the yeast proteome by systematic analysis of protein complexes. *Nature* 415, 141–147 (2002). [PubMed: 11805826]
14. Krogan NJ et al. Global landscape of protein complexes in the yeast *Saccharomyces cerevisiae*. *Nature* 440, 637–643 (2006). [PubMed: 16554755]
15. Yu H et al. High-quality binary protein interaction map of the yeast interactome network. *Science* 322, 104–110 (2008). [PubMed: 18719252]
16. Tarassov K et al. An *in vivo* map of the yeast protein interactome. *Science* 320, 1465–1470 (2008). [PubMed: 18467557]
17. Zhu J et al. Integrating large-scale functional genomic data to dissect the complexity of yeast regulatory networks. *Nat. Genet.* 40, 854–861 (2008). [PubMed: 18552845]
18. Bender A & Pringle JR Multicopy suppression of the *cdc24* budding defect in yeast by *CDC42* and three newly identified genes including the *ras*-related gene *RSR1*. *Proc. Natl. Acad. Sci. USA* 86, 9976–9980 (1989). [PubMed: 2690082]
19. Shimada Y, Wiget P, Gulli MP, Bi E & Peter M The nucleotide exchange factor *Cdc24p* may be regulated by auto-inhibition. *EMBO J.* 23, 1051–1062 (2004). [PubMed: 14988726]

20. Shannon P et al. Cytoscape: a software environment for integrated models of biomolecular interaction networks. *Genome Res.* 13, 2498–2504 (2003). [PubMed: 14597658]
21. van Dongen S A Cluster Algorithm for Graphs (National Research Institute for Mathematics and Computer Science in The Netherlands, Amsterdam, 2002).
22. Myers CL, Barrett DR, Hibbs MA, Huttenhower C & Troyanskaya OG Finding function: evaluation methods for functional genomic data. *BMC Genomics* 7, 187 (2006). [PubMed: 16869964]
23. Ma H, Kunes S, Schatz PJ & Botstein D Plasmid construction by homologous recombination in yeast. *Gene* 58, 201–216 (1987). [PubMed: 2828185]
24. Ho CH et al. A molecular barcoded yeast ORF library enables mode-of-action analysis of bioactive compounds. *Nat. Biotechnol.* 27, 369–377 (2009). [PubMed: 19349972]
25. De Wulf P, McAinsh AD & Sorger PK Hierarchical assembly of the budding yeast kinetochore from multiple subcomplexes. *Genes Dev.* 17, 2902–2921 (2003). [PubMed: 14633972]
26. Pagliuca C, Draviam VM, Marco E, Sorger PK & De Wulf P Roles for the conserved spc105p/kre28p complex in kinetochore-microtubule binding and the spindle assembly checkpoint. *PLoS ONE* 4, e7640 (2009). [PubMed: 19893618]
27. Pramila T, Wu W, Miles S, Noble WS & Breeden LL The Forkhead transcription factor Hcm1 regulates chromosome segregation genes and fills the S-phase gap in the transcriptional circuitry of the cell cycle. *Genes Dev.* 20, 2266–2278 (2006). [PubMed: 16912276]
28. Balciunas D & Ronne H Yeast genes GIS1–4: multicopy suppressors of the Gal-phenotype of *snf1 mig1 srb8/10/11* cells. *Mol. Gen. Genet.* 262, 589–599 (1999). [PubMed: 10628841]
29. Li JM, Li Y & Elledge SJ Genetic analysis of the kinetochore DASH complex reveals an antagonistic relationship with the ras/protein kinase A pathway and a novel subunit required for Ask1 association. *Mol. Cell. Biol.* 25, 767–778 (2005). [PubMed: 15632076]
30. Tanaka K & Hirota T Chromosome segregation machinery and cancer. *Cancer Sci.* 100, 1158–1165 (2009). [PubMed: 19432891]
31. Toda T et al. Cloning and characterization of BCY1, a locus encoding a regulatory subunit of the cyclic AMP-dependent protein kinase in *Saccharomyces cerevisiae*. *Mol. Cell. Biol.* 7, 1371–1377 (1987). [PubMed: 3037314]
32. Klein HL Spontaneous chromosome loss in *Saccharomyces cerevisiae* is suppressed by DNA damage checkpoint functions. *Genetics* 159, 1501–1509 (2001). [PubMed: 11779792]
33. Hodgkin J Genetic suppression. *WormBook* 27, 1–13 (2005).
34. Reed SI, Hadwiger JA, Richardson HE & Wittenberg C Analysis of the Cdc28 protein kinase complex by dosage suppression. *J. Cell Sci. Suppl* 12, 29–37 (1989). [PubMed: 2699737]
35. Wittenberg C, Sugimoto K & Reed SI G1-specific cyclins of *S. cerevisiae*: cell cycle periodicity, regulation by mating pheromone, and association with the p34CDC28 protein kinase. *Cell* 62, 225–237 (1990). [PubMed: 2142620]
36. Aalto MK, Ronne H & Keranen S Yeast syntaxins Sso1p and Sso2p belong to a family of related membrane proteins that function in vesicular transport. *EMBO J.* 12, 4095–4104 (1993). [PubMed: 8223426]
37. Watts FZ, Shiels G & Orr E The yeast MYO1 gene encoding a myosin-like protein required for cell division. *EMBO J.* 6, 3499–3505 (1987). [PubMed: 3322809]
38. Rodriguez-Quinones JF et al. Global mRNA expression analysis in myosin II deficient strains of *Saccharomyces cerevisiae* reveals an impairment of cell integrity functions. *BMC Genomics* 9, 34 (2008). [PubMed: 18215314]
39. Mani R, St. Onge RP, Hartman JLIV, Giaever G & Roth FP Defining genetic interaction. *Proc. Natl. Acad. Sci. USA* 105, 3461–3466 (2008). [PubMed: 18305163]
40. St. Onge, R.P. et al. Systematic pathway analysis using high-resolution fitness profiling of combinatorial gene deletions. *Nat. Genet.* 39, 199–206 (2007). [PubMed: 17206143]
41. Gasch AP et al. Genomic expression programs in the response of yeast cells to environmental changes. *Mol. Biol. Cell* 11, 4241–4257 (2000). [PubMed: 11102521]
42. Gordon CL & King J Genetic properties of temperature-sensitive folding mutants of the coat protein of phage P22. *Genetics* 136, 427–438 (1994). [PubMed: 8150274]

43. Warner JR & McIntosh KB How common are extraribosomal functions of ribosomal proteins? *Mol. Cell* 34, 3–11 (2009). [PubMed: 19362532]
44. Haarer B, Viggiano S, Hibbs MA, Troyanskaya OG & Amberg DC Modeling complex genetic interactions in a simple eukaryotic genome: actin displays a rich spectrum of complex haploinsufficiencies. *Genes Dev.* 21, 148–159 (2007). [PubMed: 17167106]
45. Komili S, Farny NG, Roth FP & Silver PA Functional specificity among ribosomal proteins regulates gene expression. *Cell* 131, 557–571 (2007). [PubMed: 17981122]
46. Ben-Aroya S et al. Toward a comprehensive temperature-sensitive mutant repository of the essential genes of *Saccharomyces cerevisiae*. *Mol. Cell* 30, 248–258 (2008). [PubMed: 18439903]
47. Li Z et al. Systematic exploration of essential yeast gene function with temperature-sensitive mutants. *Nat. Biotechnol.* 29, 361–367 (2011). [PubMed: 21441928]
48. Maere S, Heymans K & Kuiper M BiNGO: a Cytoscape plugin to assess overrepresentation of gene ontology categories in biological networks. *Bioinformatics* 21, 3448–3449 (2005). [PubMed: 15972284]
49. Butcher RA & Schreiber SL A microarray-based protocol for monitoring the growth of yeast overexpression strains. *Nat. Protoc.* 1, 569–576 (2006). [PubMed: 17406283]
50. Pierce SE et al. A unique and universal molecular barcode array. *Nat. Methods* 3, 601–603 (2006). [PubMed: 16862133]
51. Lea DE & Coulson CA The distribution of the numbers of mutants in bacterial populations. *J. Genet.* 49, 264–285 (1949). [PubMed: 24536673]

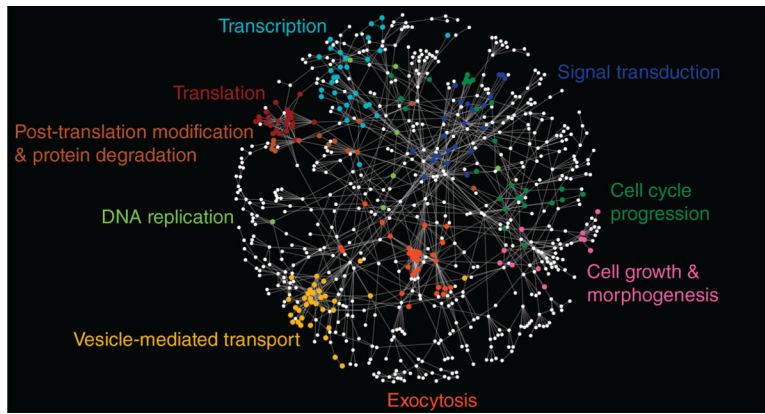


Figure 1.

Dosage suppression genetic interaction network for *S. cerevisiae*. Network diagram of dosage suppression genetic interactions. Genes are represented as nodes and interactions are represented as edges. Colored nodes are sets of genes enriched for Gene Ontology biological processes summarized by the indicated terms. The nodes were distributed using a force-directed layout, such that genes (nodes) that share common dosage suppression interactions form distinct clusters.

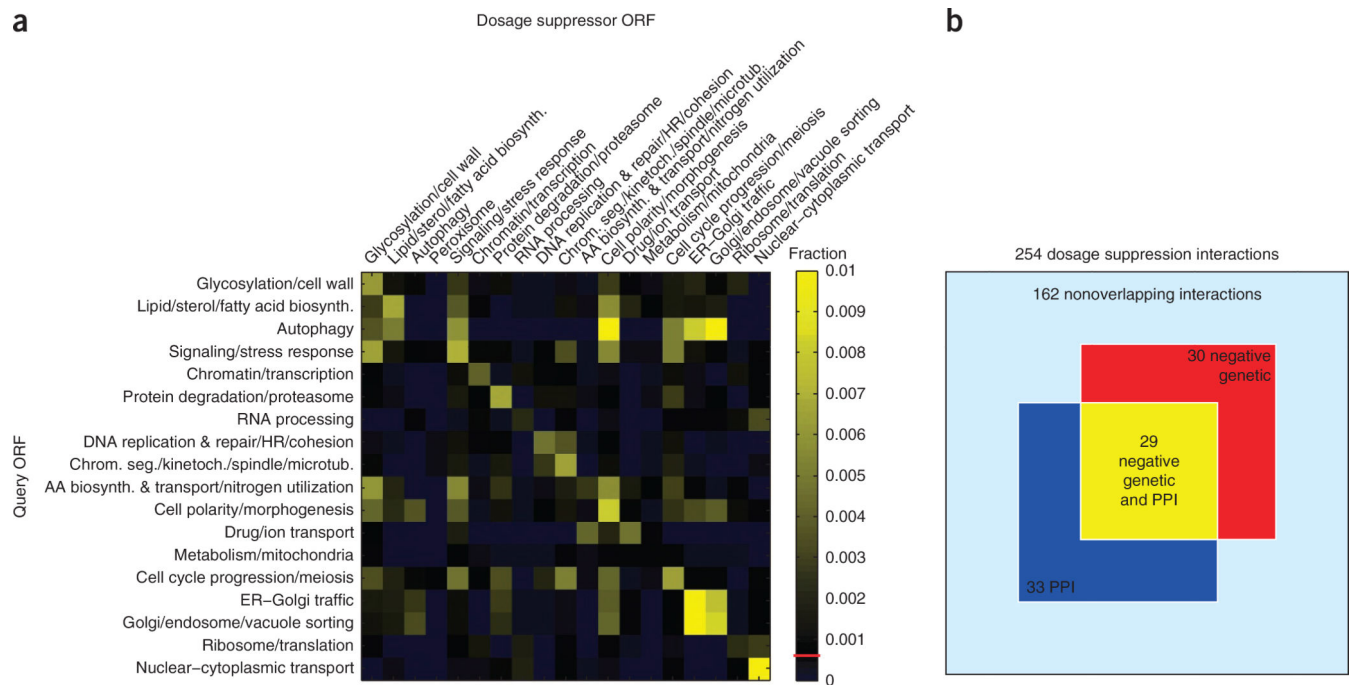


Figure 2.

Properties of the yeast dosage suppression network. **(a)** Frequency of dosage suppression genetic interactions within and across biological processes for the dosage suppression network. The frequency of gene pairs showing dosage suppression interactions was measured for 19 broadly defined functional gene sets¹¹; blue, less than the frequency of random pairs; black, statistically indistinguishable from a random set of gene pairs; yellow, greater than the frequency of random pairs. Dosage suppressor gene function. *x* axis; query ORF gene function, *y* axis. The diagonal represents within-process interactions. Red line in color scale, frequency of interactions expected by chance (0.0005). **(b)** Scaled square Venn diagram of fraction of dosage suppression gene pairs that also show negative genetic and protein-protein interactions (PPI). Only gene pairs known to be tested for both genetic and physical interactions were considered. Light blue, gene pairs showing dosage suppression interactions only; red, gene pairs showing dosage suppression and negative genetic interactions; dark blue, gene pairs showing dosage suppression and physical interactions; yellow, gene pairs showing dosage suppression, negative genetic and physical interactions.

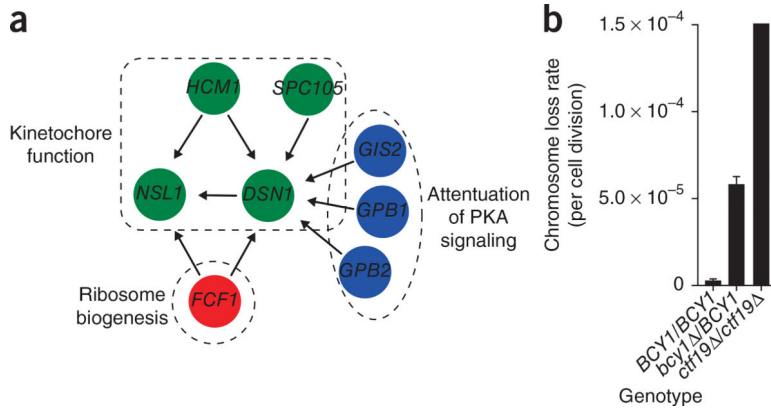


Figure 3. A genetic requirement for PKA signaling in kinetochore function. (a) Subset of results of using MoBY-ORF 2.0 to screen for dosage suppressors of *NSL1* or *DSN1*, two components of the MIND kinetochore complex. Arrows link suppressors to the mutated gene. Green, kinetochore function; blue, PKA signaling; red, ribosome biogenesis. (b) Attenuation of PKA signaling may be required for proper kinetochore function. Fluctuation tests were carried out to measure chromosome loss rates with freshly grown diploid colonies of each genotype as described³². Values are mean ± s.d. *n* = 3 for *BCY1/BCY1* and *bcy1 /BCY1*, *n* = 2 for *ctf19 /ctf19* .

Author Manuscript

Author Manuscript

Author Manuscript

Author Manuscript

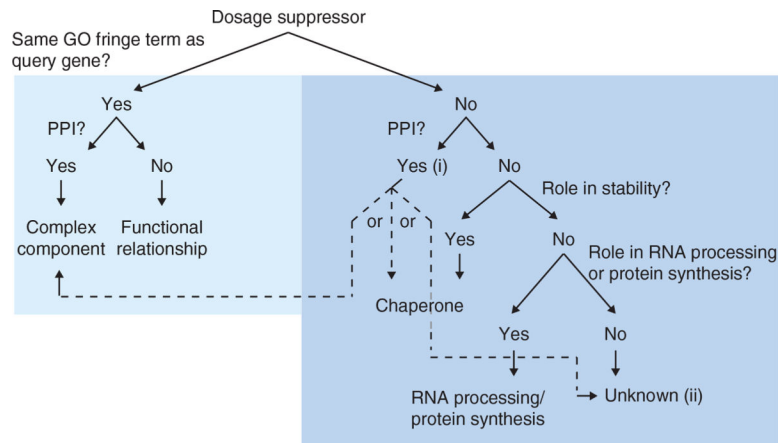


Figure 4.

Decision tree used to categorize dosage suppression interactions. Dosage suppression gene pairs were classified into one of four mechanistic categories. First, gene pairs were analyzed to see if they were annotated with the same Gene Ontology term and/or were also linked by a protein-protein interaction. Gene pairs that did not fit into either of these categories were mechanistically categorized as a chaperone, an RNA processing/ protein synthesis dosage suppressor or an unknown dosage suppressor. A chaperone is a dosage suppressor that encodes a gene required for RNA or protein stability, such as a heat-shock protein, that might act to stabilize the mutant query gene product. A dosage suppressor can also participate in RNA processing or protein synthesis. For gene pairs that could otherwise not be classified because their gene products physically interacted but the genes themselves were not functionally related (i), we found additional evidence supporting a functional relationship by examining the primary literature (dotted arrows). Thirteen percent of all gene pairs could not be classified and fell into a category labeled unknown (ii).

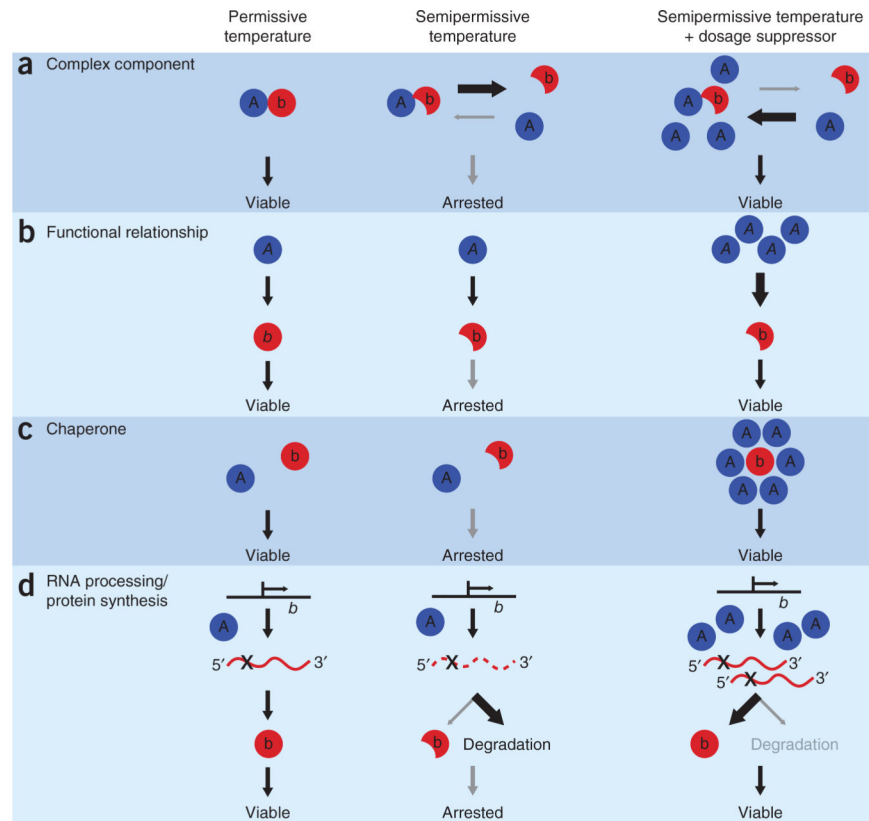


Figure 5. Mechanisms of dosage suppression in yeast. **(a)** Complex component. A dosage suppressor can be a gene that encodes a protein that interacts with the mutant gene product and is required for its normal function. At the semipermissive temperature, the mutant protein *b* predominantly occurs in an unfolded state, probably because the mutation renders the gene product unstable, and it therefore cannot interact with its normal physical partner(s). Overexpression of a dosage suppressor, protein *A*, increases amount of properly folded mutant protein so that the physical complex can execute its essential function. **(b)** Functional relationship. A dosage suppressor can function either upstream or downstream of its respective mutant query allele in the same biological process. In this example, at the semipermissive temperature, the function of the mutant allele *b* gene product is impaired and cannot transmit information to a downstream effector. A dosage suppressor, encoded by gene *A*, can act upstream of the mutant allele to activate the pathway. **(c)** Chaperone. A dosage suppressor can affect the amount of the mutant gene product. In this example, the dosage suppressor protein does not normally interact with the mutant gene product. At the semipermissive temperature, the mutant protein *b* is unfolded, but overexpression of a dosage suppressor, such as a chaperone (protein *A*), can refold and stabilize the mutant protein, enabling it to carry out its essential function. **(d)** RNA processing/protein synthesis. A dosage suppressor can be a gene that acts during transcription or translation. In this example, the dosage suppressor protein *A* is normally involved in some aspect of transcription. At the semipermissive temperature, transcription of mutant allele *b* leads to a poor-quality mRNA product that may be translated but probably will be degraded. By

increasing some aspect of transcription, however, it might be possible to improve the quality of the mRNA product, which can then be translated instead of degraded, leading to enough functional mutant protein for the cell to be viable.

Author Manuscript

Author Manuscript

Author Manuscript

Author Manuscript

Table 1

Overlap of dosage suppression interactions with other types of interactions

Type of interaction	Dosage suppression (SGD)		Dosage suppression (this study)		P value ^a
	No. tested pairs	No. overlapping pairs	No. tested pairs	No. overlapping pairs	
Physical	1,503 ^b	525	150	27	$\ll 10^{-16}$
Negative genetic	254 ^c	59	57 ^c	8	1.03×10^{-5}
Positive genetic	254 ^c	4	57 ^c	0	N/A

^aP-values based on a hypergeometric test.^bQuery-dosage suppressor gene pairs annotated in the SGD as 'dosage rescue' in which the bait is an essential gene (Supplementary Table 1).^cSubset of query-dosage suppressor gene pairs (Supplementary Table 1) that have been screened for genetic interactions¹¹.